

Calibration of Meteor Spectra

Martin Dubs¹ and Koji Maeda²

¹FMA (Fachgruppe Meteorastronomie), Maienfeld, Switzerland

martin-dubs@bluewin.ch

²Nippon Meteor Society and University of Miyazaki, Miyazai, Japan

mae@mrf.biglobe.ne.jp

Meteor spectra give valuable information about the composition of meteors. The nonlinear dispersion of spectra together with the motion of the meteors complicates the analysis. In this presentation a simple method to calibrate spectra in wavelength and flux is presented. By an image transformation to an orthographic projection the dispersion becomes linear and the curved spectra become straight and parallel. The resulting spectra, after suitable pre-processing, can be analyzed with standard spectroscopy software.

1 Introduction

The widespread use of high sensitivity video cameras has lead to an increased interest in meteor spectroscopy. However the calibration and analysis of spectra has been done by only a few experts, mainly because of the nonlinear dispersion of the spectra, which complicates the calibration. The appearance of meteors anywhere in the field of view and their rapid movement pose additional challenges for the analysis. Most spectra are recorded with diffraction gratings as a dispersion element. In this talk a method is described which allows to transform the nonlinear curved spectra into linear, straight spectra parallel to the main dispersion direction of the grating. All the meteor spectra images are transformed to a orthographic projection. This is done by image transformation software similar to the software used to correct lens distortion. Linear spectra with constant dispersion have the advantage that they can be stacked and processed with standard spectroscopy software used for stellar spectra.

Wavelength calibration is the main topic, however some points on intensity calibration are also highlighted. In order to achieve high numbers of meteor spectra, lenses with a wide field of view are often used. These show vignetting in the corners, which has to be corrected in addition to the correction caused by the image transformation. Often overlooked is the angle dependence of the grating efficiency. The effect of atmospheric extinction should not be neglected, ideally by calibrating the spectra with close by reference stars.

2 Linearization of wavelength scale

As can be seen in Figure 1, meteor spectra show a nonlinear wavelength scale, the dispersion measured in pixel/nm varies as a function of wavelength and meteor position. This can also be seen from the grating equation (Schroeder, 1970):

$$m\lambda G = (\sin \alpha + \sin \beta) \cos \gamma \quad (1)$$

where m is the grating order, G the number of grooves/mm, α the incidence angle, β the exit angle of the

light onto the grating and γ the out of plane angle from the grating normal. In addition, the spectra are curved, which further complicates the analysis.

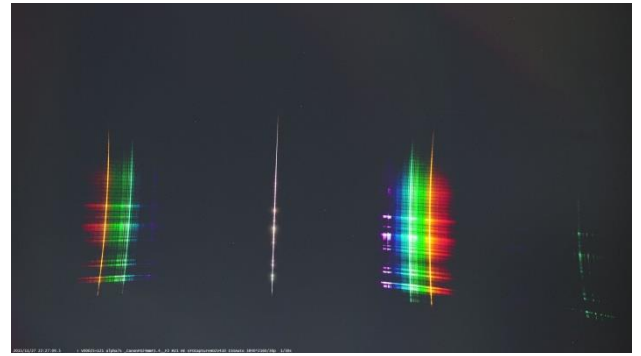


Figure 1, original meteor spectrum, recorded by Koji Maeda, 20151127_222709, Sony alpha 7S, f 24mm, grating 600L/mm
For the present discussion a different set of equations, given by Rowland (1893), is more useful. Using vector notation for the incident and diffracted ray, the following equations are obtained for the components of unit vectors:

$$A' = A + m\lambda G \quad (2)$$

$$B' = B \quad (3)$$

$$C' = \sqrt{(1 - A'^2 - B'^2)} \quad (4)$$

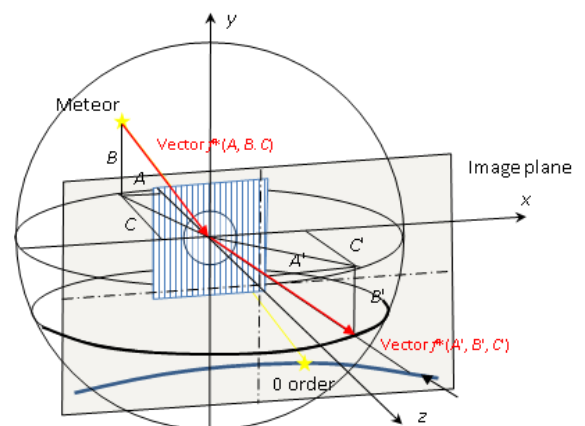


Figure 2, vector components of incident and diffracted ray

The important point is that (2) is linear in wavelength, the component B' is constant and the nonlinearity is only in (4), which is used to calculate the position of the spectrum in the CCD plane (the resulting spectrum in the CCD plane has the shape of a hyperbola).

The idea is now to transform the CCD images of the spectra and transform them to coordinates A' and B', linear in wavelength or in other words, to transform the gnomonic projection (central perspective of a sphere onto a plane) into an orthographic projection (parallel projection of a sphere onto a plane). In this transformation the correction of lens distortion can be easily included, if the grating is oriented perpendicular to the optical axis of the lens. Details are given in Dubs and, Schlatter (2015). The required transformation maps a point in the original image, $P = (r, \varphi)$, to a point in the radially modified image, $P' = (r', \varphi)$, where the coordinates are measured from the optical axis. For the transformation a polynomial equation of the following form is used:

$$r = f(r'/f + a_3(r'/f)^3 + a_5(r'/f)^5 + \dots) = r'(1 + a_3(r'/f)^2 + a_5(r'/f)^4 + \dots) \quad (5)$$

(f is the focal length of the lens, in the centre the scale is not changed, a_3 and a_5 are polynomial coefficients). The coefficients are determined by recording the spectrum of a calibration light in different areas of the image and fitting the spectrum positions to the linear calculated positions by a least square fit. Fortunately this has to be done only once for each grating – lens combination. After the transformation all the spectra are parallel (a rotation has been included to make them horizontal) and the dispersion is constant everywhere in the image (which can be checked by measuring the constant separation of the negative and positive 1st order and the 2nd order of the Mg line):

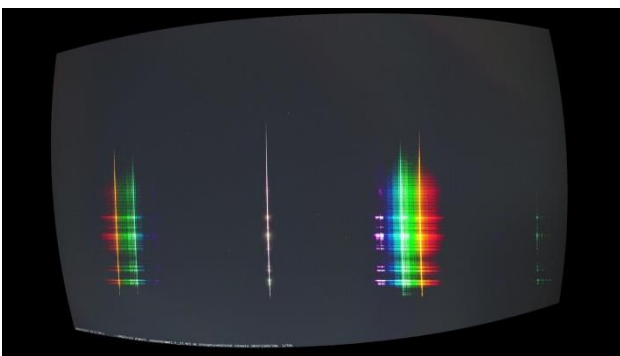


Figure 3, meteor spectrum of figure 1 after image transformation and rotation

In a colour spectrum the identification of the different lines and orders is easy. The constant dispersion helps in identifying unknown lines in black and white spectra if a single line is identified, even if the zero order is missing. Wavelength differences are obtained by multiplying the separation in pixels with the known dispersion.

3 Processing of spectra

In order to extract a useful spectrum or a series of spectra at different times the images need some processing to

remove background, correct for vignetting and align them. This is done in a similar way to the processing of stellar images, with the difference that the meteor is moving fast, so some extra step has to be taken to freeze its movement. The processing can be separated into three stages, first the preprocessing, then the image transformation and third the extraction of the spectra. It is shown for the case of video observation, for long time exposure the processing would be somewhat different.

Preprocessing

This consists of extracting the images from the video stream, removal of background and correcting for vignetting. Fortunately sky brightness and stars are constant over short periods, so a background image can be calculated as the average of images before the appearance of the meteor and subtracted from the meteor images.

The vignetting is particularly noticeable with wide angle lenses. A flat image can be recorded of a white screen (a foggy sky or a twilight flat serves the same purpose) without grating. Figure 4 shows an extreme example.



Figure 4, flat image of Canon EOS6d with lens Sigma 35mm, f/1.4

The background corrected images are divided by the flat image to correct for the vignetting¹.

Image transformation

The image transformation to the orthographic projection has been described above. It is done by software similar to that used for correcting lens distortion². By an additional rotation the spectra can be oriented parallel to the horizontal axis. This simplifies the extraction of the spectrum.

Extraction of spectra

After the image transformation all the spectra have a constant dispersion (the same scale in nm/pixel) and are

¹ An additional correction by a factor $1/\cos(\rho)$ is necessary to take into account the change of scale from an equal area projection to the orthographic projection ($\rho = \arcsin(r'/f)$), in order to preserve photon flux. This can be included in the flat correction. A different flat correction is needed without the image transformation, since a gnomonic projection also changes equal areas on the sky to different areas on the CCD. A flat correction may do more harm in that case.

² In the present work a specially adapted software ImageTools by Peter Schlatter has been used.

aligned parallel. They may be shifted to a fixed position of the zero order and stacked for increase of S/N. Alternatively they can be processed image by image and displayed as a time series. The intensities of the rows containing the spectrum are added column by column. Next the pixel scale is converted to wavelength with a linear transformation, using the zero order as origin or a known line (e.g. the Na line) as a wavelength reference, in case the zero order is out of the image area. The linearity may be checked with some known other lines or higher orders.

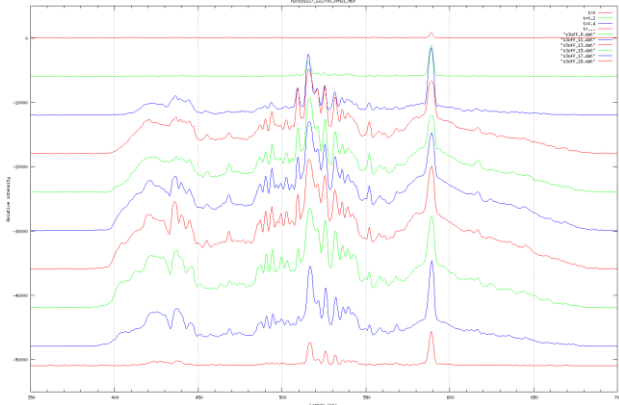


Figure 5, wavelength calibrated time series of spectra for meteor of figure 1, time interval 0.2 sec top to bottom, notice saturation of strong lines

4 Flux calibration

For many purposes this wavelength calibrated spectrum is sufficient. For a quantitative analysis of line strengths a calibration of the intensity is required. In most cases a relative calibration of intensities is sufficient. The principal factors affecting calibration are the wavelength dependence of:

- Atmospheric extinction
- Grating efficiency
- Lens transmissivity
- Sensor sensitivity or quantum efficiency

It is not possible to give a full discussion, so some points of special interest in meteor spectroscopy will be highlighted.

Atmospheric transmission follows the extinction law (Appenzeller, 2013):

$$T_a(\lambda) \approx \exp[-\tau(\lambda)/\cos(z)] \quad (6)$$

with $\tau(\lambda)$ the optical depth of the atmosphere in the zenith. z is the zenith distance. A precise determination would require a determination of the atmospheric extinction at the time of the meteor apparition, in practice one can use a standard curve for the time of observation.

Grating efficiency curves can be obtained from the grating manufacturer. Note however that this function is measured or calculated only for normal incidence of the light. The efficiency of a blazed grating is very sensitive

to the incidence angle α , as the following diagram shows for a 600 L/mm grating with a blaze angle of 28.7° .³

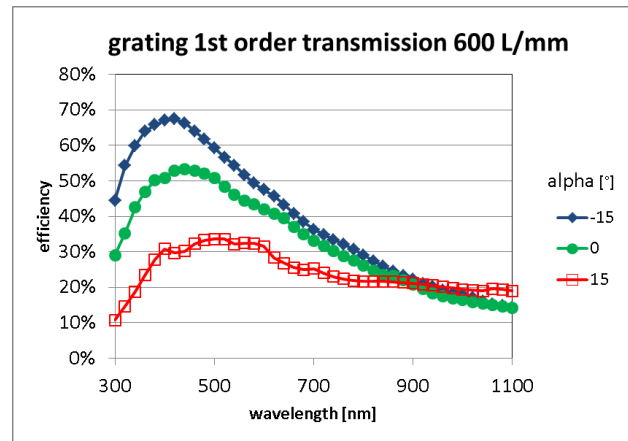


Figure 6, grating efficiency of a 600 L/mm grating, calculated for 1st order for different incidence angles

For other orders the angle and wavelength dependence is even more severe, so an intensity correction is normally not done. In a standard slit spectrograph you do not have this problem, since the incident angle is fixed by the grating orientation and slit position.

The sensor sensitivity can be taken from the manufacturer datasheet, note that a factor proportional to λ enters for the conversion from photon number to photon energy.

The instrument response is finally calculated by multiplying all these factors. Since some of these are not precisely known (atmosphere, additional windows, lens transmission) a more practical way is to determine the instrument response by measuring a standard star and dividing its spectrum by the known spectral flux of this star. A good source for calibration spectra is e.g. the Miles database.⁴ This can be improved by taking into account the differential atmospheric extinction with (6).

Practical considerations

For color images with a Bayer matrix a correction with the instrument response is not advisable because of the low sensitivity at the short and long wavelength limit and the irregular shape of the response function, modified by the filter transmission of the color filters. For that reason the following example is for a Watec 902H2 ultimate camera with a 600 L/mm grating. The instrument response $IR(\lambda)$ was determined with a reference star. Venus was in a good position in the sky at the time of the meteor.

$$IR(\lambda) = \langle I_{meas}(\lambda) / F_{ref}(\lambda) \rangle \quad (7)$$

The measured spectrum of the reference star is divided by the flux of the reference and suitably smoothed. The measured spectrum of the meteor is then flux corrected by multiplying with the IR. By carefully keeping track of

³ Calculated with Gsolver V4.20b, <http://www.gsolver.com/>

⁴ <http://www.iac.es/proyecto/miles/>

normalization factors an absolute flux of the meteor may be calculated with the same equations.

$$Flux_{Met}(\lambda) = I_{Met}(\lambda)/IR(\lambda) \quad (8)$$

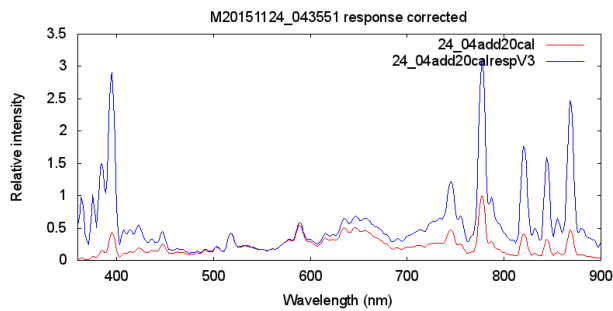


Figure 7, meteor spectrum recorded with Watec902H2 ultimate, red: original, blue: instrument response corrected

5 Equipment

Some words about the equipment used in these tests and the results obtained so far are useful. The first experiments were done with a Video camera Watec 902H2 ultimate with a Tamron 12VG412ASIR ½", f: 4-12mm f/1.2 lens, operated at $f \cong 7\text{mm}$, with a Thorlabs grating with 300 grooves/mm, exchanged for a grating with 600 grooves/mm (see figure 7). In first order this gives an inverse dispersion of 2.0 nm/pixel, which is about the minimum of usability. In addition the 8-bit readout limits the dynamic range. Unfortunately meteors do not appear with the correct intensity to make best use of this range, so they are either underexposed with a poor S/N ratio or overexposed, saturating the strong lines which make them unusable for quantitative analysis. Occasionally some video frames with the correct intensity can be used, but then much information about the temporal behaviour gets lost.

The color spectra have been recorded with a Sony alpha 7s, f 24mm, or a Canon EOS6D with lens Sigma 35mm, F/1.4, both with a grating 600 grooves/mm. These record in 3x8-bit color mode. The larger chip size allows higher dispersion (0.62 nm/pixel for the Sony alpha at full resolution of 3840x2160 and 1.06 nm/pixel with the Canon at a resolution of 1920x1080). Unfortunately the Bayer matrix reduces the sensitivity, complicates the analysis and makes quantitative analysis unreliable. The 8-bit readout again is a limiting factor for the quantitative analysis.

A really useful camera for meteor spectroscopy should have a large chip, 12- or 16-bit monochrome readout at around 30 frames/second and an affordable price. Unfortunately these requirements are somewhat contradictory.

6 Conclusions

This work shows that the analysis of meteor spectra can be simplified by the transformation of the images to an orthographic projection. The resulting spectra have a

constant dispersion and are parallel for any position of the meteor. They can be analyzed with standard spectroscopy



Figure 8, Sony alpha7s equipped with grating 600 grooves/mm software. In the future it is planned to simplify the calibration and to streamline the processing pipeline. This may help in popularizing meteor spectroscopy in the community. At present additional stations of the FMA plan the installation of meteor spectroscopy cameras in Switzerland. Since two years the FMA operates a network of video, fireball detection, radar and seismic stations, which in combination allow a better characterisation of meteors.

Acknowledgment

M. D. thanks the FMA (Fachgruppe Meteorastronomie) for providing data and helpful discussions, in particular Peter Schlatter for his assistance with software, Roger Spinner and Jonas Schenker for the meteor database and webpage⁵, where the results of meteor spectroscopy are presented.

References

- Appenzeller I. (2013), Introduction to Astronomical Spectroscopy, Cambridge University Press, p174
- Dubs, M. and Schlatter, P. (2015), A practical method for the analysis of meteor spectra, WGN, the Journal of the IMO 43:4, p94
- Rowland H. A. (1893), Gratings in Theory and Practice, Astron. and Astrophys, Vol 12, p129
- Schroeder D. J. (1970), Design considerations for astronomical echelle spectrograph, PASP, Vol82, No490, p1253

⁵ <http://www.meteorastronomie.ch/>